Payload study activities on the International X-ray Observatory

D. Martin[a], N. Rando[a], D. Lumb[a], P. Verhoeve[a], T. Oosterbroek[a], L. Puig[a], G. Saavedra[a], M. Bavdaz[a] and P. Gondoin[a]
[a]ESA-ESTEC, Keplerlaan 1, 2200 AG Noordwijk ZH, The Netherlands

ABSTRACT

The International X-ray Observatory (IXO) is an L class mission candidate within the science programme Cosmic Vision 2015-2025 of the European Space Agency, with a planned launch by 2020. IXO is an international cooperative project, pursued by ESA, JAXA and NASA. By allowing astrophysical observations between 100 eV and 40 keV using a very large effective collecting area mirror and state-of-the art instruments, IXO would represent the new generation X-ray observatory, following the XMM-Newton, Astro-H and Chandra heritage.

The IXO mission concept is based on a single aperture telescope with an external diameter of about 3.5 m and a focal length of 20 m. The focal plane consists of a fixed and a moveable instrument platform (FIP and MIP respectively). The model payload consists of a suite of five instruments which can each be located at the telescope's focus by the MIP, these are:

1. a wide field imager (WFI) based on a silicon DEPFET array;
2. a Hard-X-ray Imager (HXI), which will be integrated together with the WFI;
3. an X-ray microcalorimeter spectrometer (XMS);
4. an X-ray Polarimeter camera (X-POL) based on a gas cell with integrated anode array;
5. a High-Time Resolution Spectrometer (HTRS) based on a silicon drift detector array.

In addition, the FIP will carry a grating spectrometer (XGS) mounted in a fixed position and which will allow simultaneous observations with the on-axis instrument.

This paper provides a summary of the preliminary results achieved during the assessment activities presently ongoing at ESA. Whereas we will provide a brief overview on the overall spacecraft design, we will focus on the payload description, characteristics, the technology used and the accommodation on the instrument platform.

Keywords: X-ray, space mission, observatory, IXO, X-ray optics, X-ray instruments

1. INTRODUCTION

The International X-ray Observatory (IXO) is an international cooperative project pursued by ESA, JAXA and NASA and resulting from the merge of the previous XEUS [1] and Constellation-X [2] studies. Following this merge, IXO has become an L-class mission candidate in the ESA Cosmic Vision 2015-2025 programme [3], with a target launch by 2020. Similarly IXO is also a candidate mission submitted to the US Decadal Survey (Astro2010) [4], while it is considered as the Astro-H follow up at JAXA.

IXO is meant to become the next-generation X-ray observatory capable of addressing some of the most important themes posed by ESA's Cosmic Vision 2015-2025 science objectives, such as: a) Evolving Violent Universe (finding massive black holes growing in the centers of galaxies, and understanding how they influence the formation and growth of the host galaxy); b) Universe taking shape (studying how the baryonic component of the Universe formed large-scale structures and understanding how and when the Universe was chemically enriched by supernovae); c) Matter Under Extreme Conditions (studying how matter behaves in very strong gravity at a very high densities, such as occurs around black holes and compact objects). IXO will also help to understand the so-called Early Universe, by enabling independent measurements of dark matter and dark energy using galaxy clusters. As an observatory class mission, IXO will also be able to address a large number of additional problems in contemporary astrophysics, such as the origin of cosmic rays in Supernovae, studies of the interstellar medium, stellar mass loss and star and planet formation.

The ESA assessment activities have started in 2008, with an internal phase 0 study, performed via the ESTEC Concurrent Design Facility. In Q3/2009 two parallel competitive industrial studies were started with EADS Astrium and Thales Alenia Space and will be completed in July 2010. In order to progress the instrument definitions to the same level as the system design, a call for Declaration of Interest was sent to the ESA member states, JAXA and NASA. Following this call, eight instrument studies were selected that cover the model payload [5]. In addition, a number of technology development activities are ongoing in parallel. All study activities are geared to the L-class down-selection process of Cosmic Vision 2015-2025, planned to take place in the first half of 2011. The main IXO requirements applicable to the ESA study are summarized in Table 1.

Table 1: IXO Science Requirements

SR1	Mirror effective Area	> 2.5 m^2 at 1.25 keV with a goal of 3 m^2	Black hole evolution, large scale structure, cosmic feedback, Strong gravity, EOS Cosmic acceleration, strong gravity
SR2		> 0.65 m^2 @ 6 keV with a goal of 1 m^2	
SR3		> 150 cm^2 @ 30 keV with a goal of 350 cm^2	
SR4	Spectral Resolution [FWHM]	ΔE = 2.5 eV within 2' × 2' (0.3 – 7 keV)	Black Hole evolution, Large scale structure Missing baryons using tens of background AGN
SR5		ΔE = 10 eV within 5' × 5' (0.3 - 7 keV)	
SR6		ΔE < 150 eV at 6 keV within 18' Ø (0.1 - 15 keV)	
SR7		E/ΔE = 3000 (0.3 – 1 keV) with a collecting area of 1,000 cm^2 for point sources	
SR8		ΔE = 1 keV within 8' × 8' (10 – 40 keV)	
SR9	Angular Resolution	≤ 5" HPD (0.1 – 10 keV)	Large scale structure, cosmic feedback, black hole evolution, missing baryons
SR10		30" HPD (10 – 40 keV) with a goal of 5"	
SR11	Count Rate	1 Crab with > 90% throughput. ΔE < 150 eV @ 6 keV (0.1 – 15 keV)	Strong gravity, EOS
SR12	Polarimetry	1% MDP on 1 mCrab, 100 ksec, 3σ, 2 – 6 keV	AGN geometry, strong gravity
SR13	Astrometry	1 arcsec at 3σ confidence	Black hole evolution
SR14	Absolute Timing	100 μsec	Neutron star studies

2. SPACECRAFT CONFIGURATION

The spacecraft consists of three distinct modules, the mirror assembly (MA), the service module (SVM) and the instrument module (IM) [6]. Because of the need of a 20 m focal length and the limited space available in the launcher, the spacecraft will be folded during launch to a height of about 11 m (see Figure 1). During this time the instrument module and deployment arms will be tightly kept in place by launch lock mechanisms. Once in orbit, three mechanical arms will deploy the instrument module to its operational position, to yield a total spacecraft length of about 24 m (see Figure 2). The mirror assembly is located inside the fixed telescope metering structure and contains the X-ray optics, the associated supporting structure and thermal control hardware. It will also house the star trackers and part of the internal metrology system used to determine the exact location of the instruments with respect to the optical axis. The service module, structurally consisting of a fixed cone (telescope metering structure), forms the interface to the launcher. It will host the usual avionics components: thrusters, fuel tanks, reaction wheels, power and data handling units, batteries and communication equipment. The SVM also hosts the deployment mechanism and shroud, which protects the instruments from straylight once deployed. Particular care was taken to provide good agility to the large spacecraft, reducing the time required for re-pointing and provide a > 85% observing efficiency. The instrument module is mounted on top of the deployment arms and accommodates all the instruments. After deployment, several mechanisms on the platform allow it

to be correctly positioned along the optical axis and in focus. The instruments and instrument platform will carry fiducial lights as part of the on-board metrology system. The concept of a single aperture telescope implies that the instruments need to be individually positioned on the optical axis. The IM therefore consists of two main parts: a fixed instrument platform (FIP) and the moving instrument platform (MIP). The Thales concept of a rotating MIP can be seen in Figure 3, conversely, Astrium considered a translating platform (Figure 5).

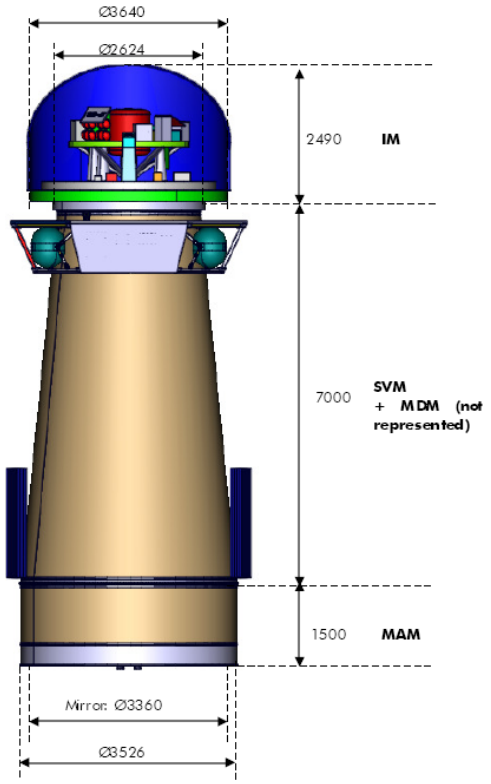

Figure 1: Stowed configuration for launch

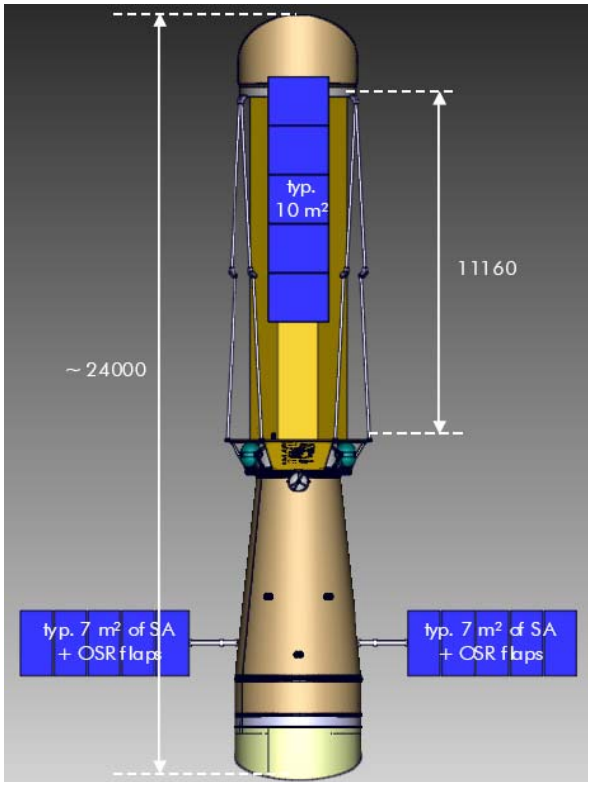

Figure 2: Deployed configuration

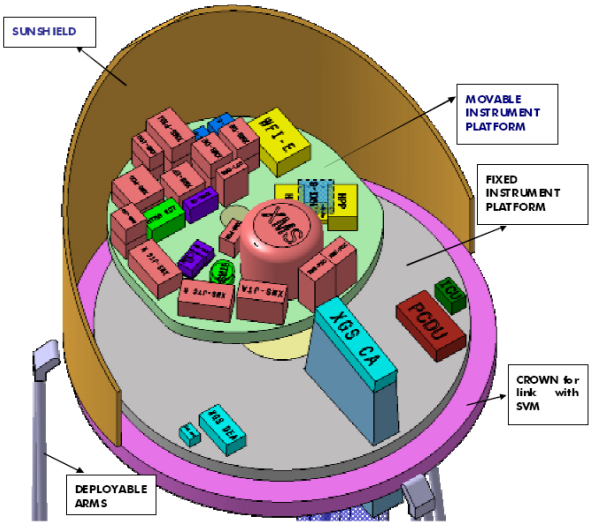

Figure 3: Thales concept of the instrument module. The MIP can rotate to place the require instrument on-axis.

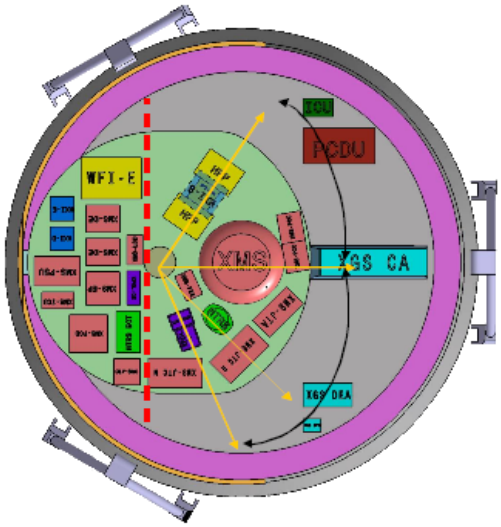

Figure 4: Top view of the instrument module. Backend electronics are mounted left of the dashed line.

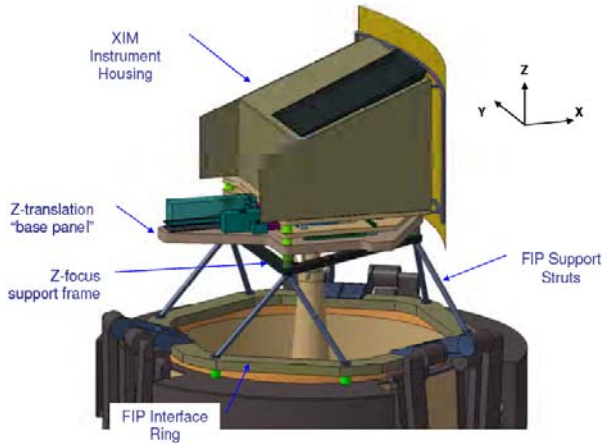

Figure 5: Astrium concept of the instrument module

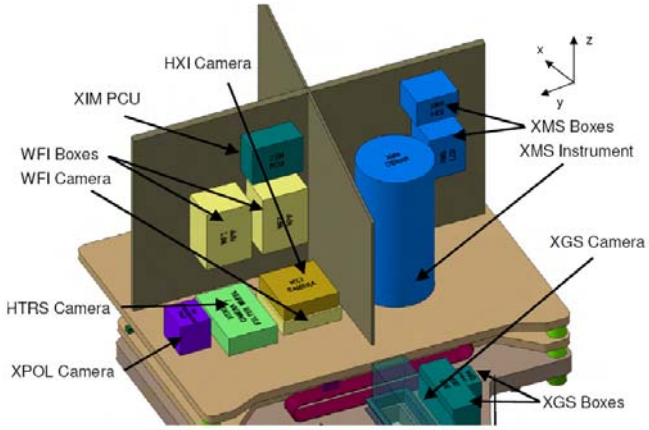

Figure 6: Instrument accommodation on the translating platform.

In order to minimize the harness routing complexity around these mechanism, all instrument boxes (except the grating camera) are mounted on the MIP. Only power and data (spacewire) cables need to be routed from MIP to FIP. Spacewire routers and a PCDU are also foreseen on the IM to minimize the data and power harnesses to the SVM.

The IM enclosure provides a protected and stable thermal environment for the instruments. The electronic boxes will be operated in an environment close to room temperature. This actually sizes the power requirements of the assembly. As instruments are switched off or placed in power saving mode when not in use, heaters need to be powered to provide the equivalent heat dissipation of the units and maintain the sub-assembly at a stable temperature. Failure to do so may require too much time for instruments to stabilize prior to being used in an observation. The detectors will all be cooled by dedicated radiators mounted on the MIP's side and top panels. The instruments will themselves provide the accurate temperature regulation of their sensor arrays.

The instrument module will also carry a sunshield, a common straylight baffle and a particle diverter. The straylight baffle is fixed to the FIP and protects the instruments from optical as well as X-ray straylight up to 70 keV. The structure of the baffle will also be used to fix the particle diverters. These magnets will deviate electrons and protons up to 21 and 75 keV respectively from the field of view of the instrument detectors. Higher energy particles, difficult to divert, will be discriminated in the instruments as they will deposit energies in their detectors in excess of the useful X-ray band-pass or be intercepted by anti-coincidence detectors.

The major issues related to the instrument accommodation that were identified and tackled during the study were: overall module mass, precision and stability of the pointing and alignment (deployment mechanism, thermo-elastic distortions) – the 1" astrometric pointing accuracy translates to 100µm at the focal plane, 20 m away from the mirror on a relatively flexible structure –, space availability on MIP to accommodate all boxes, thermal control (large dissipation in small volume), cryogenics required for the XMS, straylight rejection and contamination.

3. INSTRUMENTS

The model instrument suite consists of six instruments, which together can fulfill the science requirements summarized in Table 1 as follows:

SR4 and SR5:	X-ray Microcalorimeter Spectrometer (XMS);
SR6:	Wide Field Imager (WFI);
SR7:	X-ray Grating Spectrometer (XGS)
SR8:	Hard-X-ray Imager (HXI);
SR11:	High-Time Resolution Spectrometer (HTRS);
SR12:	X-ray Polarimeter camera (X-POL).

All instruments, except the XGS, are mounted on the MIP. The HXI camera will be mounted at the back of the WFI and will be delivered together as a single instrument. The MIP can be placed in four nominal positions, allowing each of the instruments to be placed at the focus of the telescope. The XGS camera and backend electronics are fixed to the FIP. It

will carry its own focusing mechanism to position it precisely on the Rowland circle. The XGS can be operated in parallel to any other on-axis instrument.

The following paragraphs will describe the current status of the instrument designs.

3.1 Wide Field Imager (WFI)

The purpose of the WFI is to provide images in the energy band 0.1–15 keV, simultaneously with spectrally and time resolved photon counting [7]. The detector consists of an array of DepFET (Depleted p-channel FET) active pixels integrated onto a common silicon bulk. Based on the principle of sideways depletion, these devices combine the advantages of sideway depleted silicon detectors with new benefits arising from the innovative DepFET concept.

The DEPFET is a combined detector-amplifier structure; see Figure 8 for a schematic representation. Every pixel consists of a p-channel MOSFET, which is integrated onto a fully depleted silicon bulk. With the help of an additional deep-n implantation, a potential minimum for electrons, the so-called internal gate, is generated and laterally constrained to the region below the transistor channel. Incident X-rays interact with the bulk material, and the resulting charge is separated; while holes drift to the most nearby p-contact, the electrons are collected in the internal gate of the adjacent pixels. There, their presence influences the conductivity of the MOSFET channel; sensing the increase of channel conductivity of the MOSFET is therefore a measure of the quantity of collected charge.

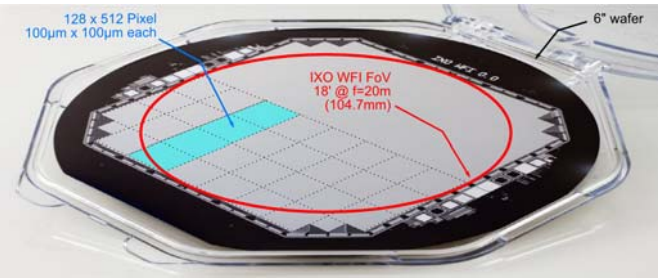

Figure 7: Full wafer WFI prototype array

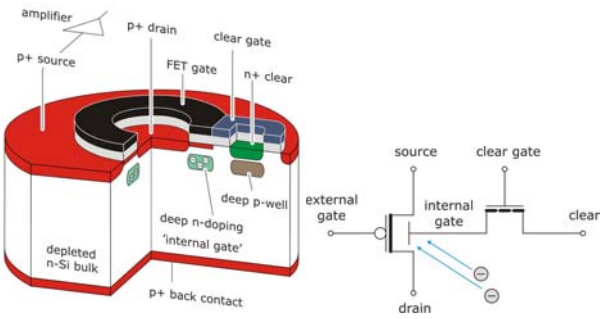

Figure 8: DepFET schematic highlighting the operating principle.

The total sensor will consist of an array of ~1024×1024 pixels, each 100×100 µm^2 monolithically integrated on a single 6" Si wafer (Figure 7), yielding a total 17.6' field of view. The sensor pixels are organized in two hemispheres of 1024×512 pixels each, which can be controlled and read out redundantly by two Hemisphere Pre-Processors (HPPs), located in close vicinity to the detector head. The HPPs control the detector array, read out the pixels, digitize and pre-processes the signals.

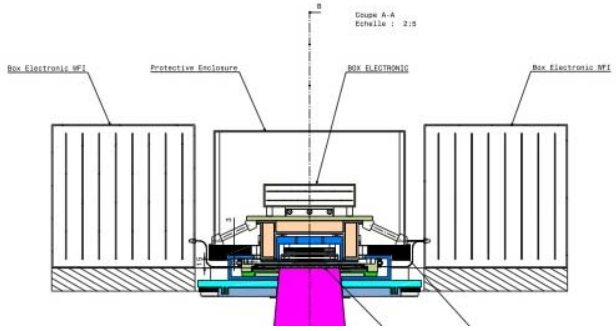

Figure 9: Combined WFI and HXI-S detector assembly.

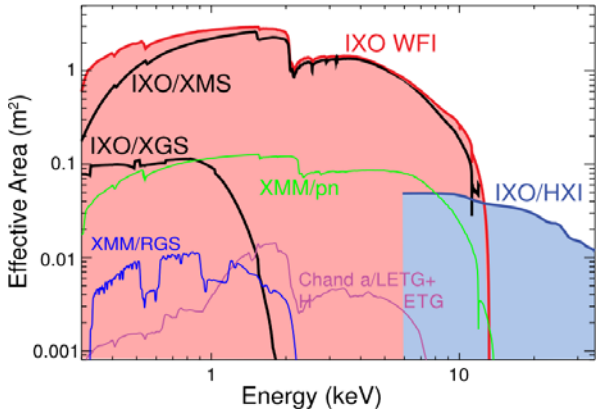

Figure 10: Comparison of the combined WFI/HXI and XGS effective areas to previous instruments.

The data from the hemisphere pre-processors is then consolidated in the Frame builder, which detects and recombines photon patterns in the pre-processed data also at the inter-hemisphere border, performs further corrections to the data and data compression for telemetry, before the data is handed to the S/C interface for telemetry. This functionality, together with the overall instrument control and power conditioning is implemented in two, redundant, instrument control and power conditioner boxes. The WFI camera head will be integrated together with the Hard X-ray Imager, described next. The soft X-rays (up to ~15keV) will predominantly be absorbed by WFI, while the harder X-rays will be detected by the HXI sensors placed directly behind the WFI, see Figure 9. The combined instrument efficiency is compared to previous generation instruments in Figure 10.

3.2 Hard X-ray Imager (HXI)

Mounted behind the WFI and operated simultaneously, the HXI will extend the energy response up to 40 keV over a field of view of 8'× 8' [8]. The detectors of the HXI will consist of two layers of double-sided Si strip detectors (DSDD) and a CdTe double-sided strip detector. The CdTe detector consists of a 2×2 arrangement of smaller detectors (Figure 11), each with 96 250 μm wide strips on either side, for a total of 768 channels. The detector assembly will be surrounded by an active BGO shield which is expected to achieve a non-X-ray background of 5×10^{-4} cts s^{-1} cm^{-2} keV^{-1}. An exploded view of the camera head is shown in Figure 12. The instrument relies heavily on Astro-H heritage, currently under development. The total HXI system is composed of three boxes, the sensor part (HXI-S), the analog electronics box (HXI-E) and the digital electronics part (HXI-D). Baffle, door and filter wheel with calibration source are shared with those of the WFI.

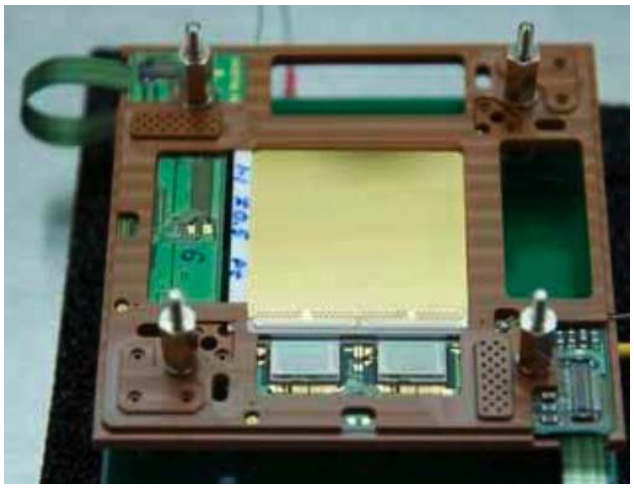

Figure 11: CdTe Strip detector, ASTRO-H heritage

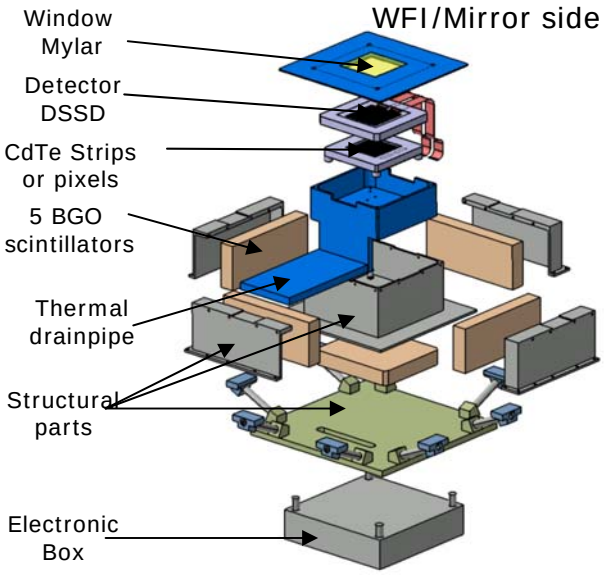

Figure 12: HXI-S detector assembly exploded view

3.3 X-ray Microcalorimeter Spectrometer (XMS)

The XMS is an imaging X-ray spectrometer based on a pixel array of micro-calorimeters [9]. It will provide images and spectra with an energy resolution of typically 2.5 eV in the energy range 0.2 – 10 keV for the central (2'×2') detector (40×40 pixels on a 300 μm pitch) and 10 eV for the wider field (5.4'×5.4') outer section (600 μm pitch pixels) with time resolved photon counting. Each pixel in the array consists of an absorber of which the temperature is read-out by a normal-to-superconducting phase transition thermometer with a critical temperature $T_c \approx 100$ mK, generally called Transition-Edge-Sensor (TES). The absorber-thermometer combination is weakly coupled to the 50 mK base temperature of the cryostat. When a photon is absorbed, the temperature increases which will result in an observable change of resistance. The resulting change in current is read-out by a Superconducting Quantum Interference Device (SQUID), acting as a current amplifier. A micrograph of a prototype for the inner array is given in Figure 13. The outer

array consist of larger absorbers (600×600 μm^2), four of which are read out by a single TES. As each absorber is linked in a slightly different matter to the TES, signals from each of them are identified by their different pulse shape.

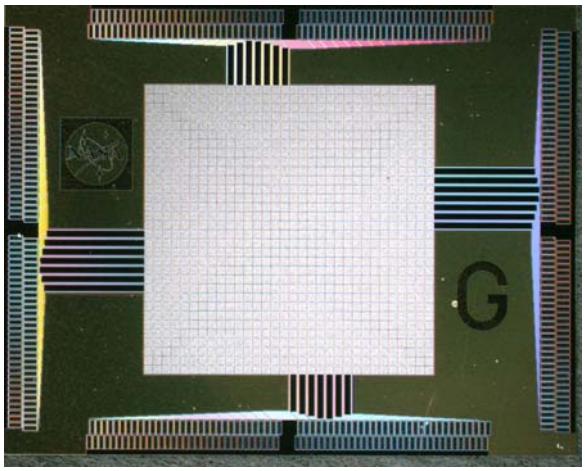

Figure 13: prototype array of 32×32 pixels

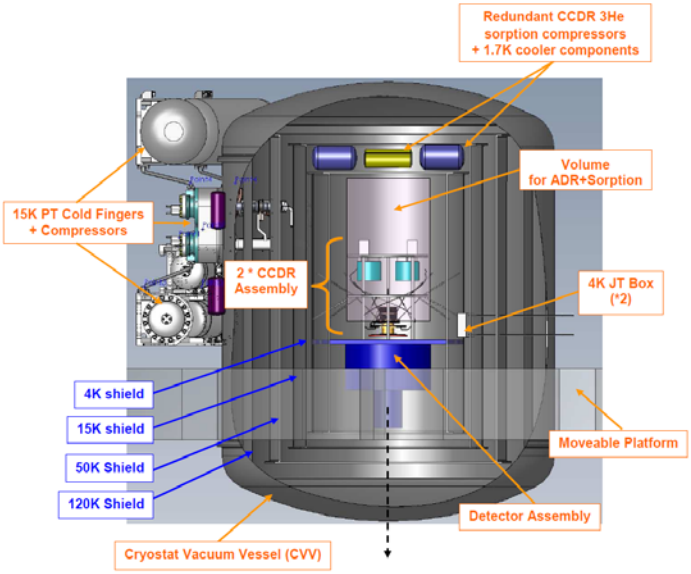

Figure 14: one of the cryostat and cooler options providing the 50mK operating temperature for the XMS detector assembly. Courtesy Air Liquide.

In order to operate the detectors, a complex and resource demanding cooling system is required to provide the 50mK interface temperature. Several different options are being developed in the USA, Japan and Europe. A possible concept, as proposed by Air Liquide, is shown in Figure 14. For lack of space we can not show here all viable alternatives, but can state that they all share the same features. The cryostat can be operated at room temperature; this relaxes the constraints of the on-ground tests. The cooling system can be separated into a pre-cooler part and a last stage cooler part, providing about 1.5 μW of cooling power at 50 mK. The pre-cooler typically consists of a 15 K double stage pulse-tube or Stirling engine, followed by a ^{4}He or ^{3}He Joule-Thomson cooler, providing a 4 K or 2 K interface to the last stage cooler respectively. These mechanical coolers will be operating continuously for the whole mission duration and have full redundancy built-in. The last stage cooler can be a single-shot system (requires recycling) which consists of either a multi-stage ADR or a hybrid sorption-ADR or can be a continuous closed-cycle dilution refrigerator.

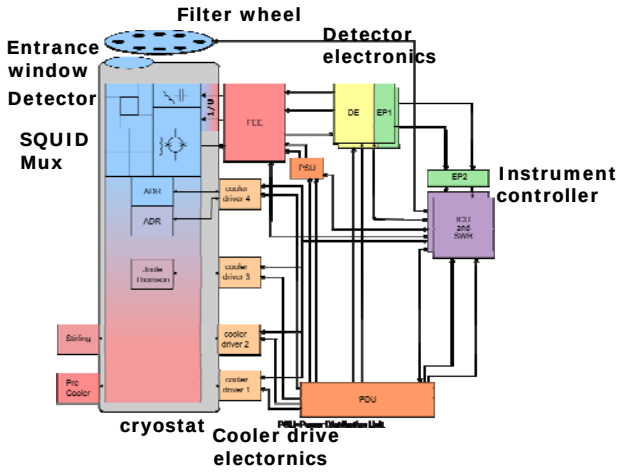

Figure 15: Overall system configuration

To overall system configuration is schematically represented in Figure 15. Detector and SQUID multiplexing are integrated in the focal plane assembly together with its magnetic shield and suspended inside the cryostat. The front-end electronics is mounted on the cryostat. Signals are sampled, de-multiplexed and filtered before being packetized by the Instrument controller.

3.4 Metal Insulator Semiconductor Microcalorimeter (MIS-XMS)

In parallel to the TESs, CEA is developing Metal-Insulator-Semiconductor (MIS) arrays. In the framework of the assessment phase, the team has investigated the impact of this design at instrument level. MIS sensors have heritage in the Herschel PACS instrument and could equally well be suited as X-ray detectors for the IXO XMS. In order to achieve the challenging energy resolution, these detectors also require to be cooled to 50 mK. The major advantage lies however in the cryogenic multiplexing and amplification stages. As the sensors have higher impedance compared to TES, they can be read out by more conventional semiconductor electronics operated at 2.5 K. Signal multiplexing is performed by a SiGe ASIC, while the pre-amplifiers are extremely low-power HEMT based circuits, see Figure 17. The power dissipation at 50mK can be substantially reduced, allowing more independent channels to be operated. The detector head consists of four quadrants (see Figure 16) of each 32×32 500µm pixel arrays, yielding a 5.5'×5.5' field of view with equal sensitivity and resolution over the whole array.

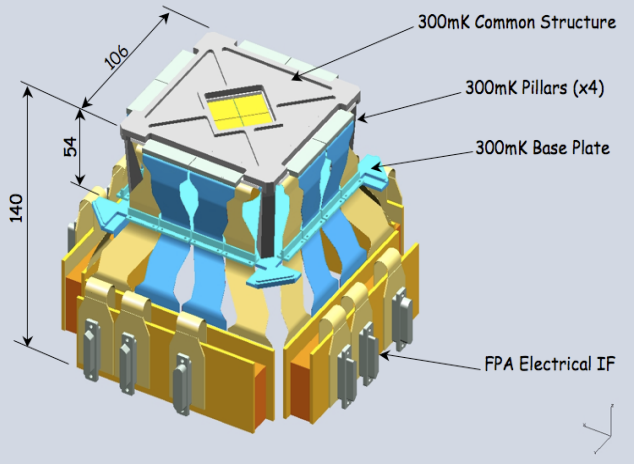

Figure 16: Detector head assembly consisting of four quadrants.

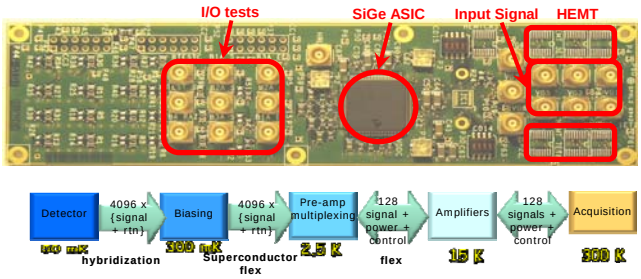

Figure 17: cryogenic electronics test board. A SiGe ASIC performs the pixel signal multiplexing and the HEMT ASIC the pre-amplification at 2.5K.

3.5 X-ray Grating Spectrometer (XGS)

The XGS is a wavelength-dispersive spectrometer for high-resolution spectroscopy in the energy band between 0.3 and 1.0 keV. It relies on a set of gratings placed between the X-ray mirror and a camera. Two concepts are being developed that will be detailed next. Both rely on the improved wavelength resolution obtained by sub-aperturing, whereby the gratings span a small fraction of the mirror in azimuth angle, exploiting the mirror modules' asymmetric PSF. The cameras are based on CCD arrays with very thin optical entrance filters to allow good efficiency at the lower X-ray energies. This, together with the larger integration time, makes the XGS the instrument most sensitive to optical straylight and sets the requirement on IXO at $< 2\times10^{8}$ photons.s^{-1}.cm^{2}. The intrinsic energy resolution of the CCDs is used to discriminate the different overlapping diffraction orders.

Critical Angle Transmission Grating (CAT-XGS)

The CAT-XGS consists of two transmission grating arrays that are placed just aft of the telescope mirrors in the convergent telescope beam, and a readout camera on the fixed instrument platform see Figures 18 and 19 [10]. The grating arrays hold a number of grating facets in a fixed position and orientation relative to the mirrors. The gratings disperse X-rays according to wavelength and focus them along a straight line (dispersion axis) into a spectrum that is recorded by the camera. The center of each grating facet touches a Rowland torus that also contains the telescope focus and the fixed blaze position in the spectrum. The CAT gratings are blazed, and therefore the diffraction efficiency is

maximized around the direction of specular reflection off the sidewall of a grating bar. The direction of specular reflection coincides with the direction of the blaze position.

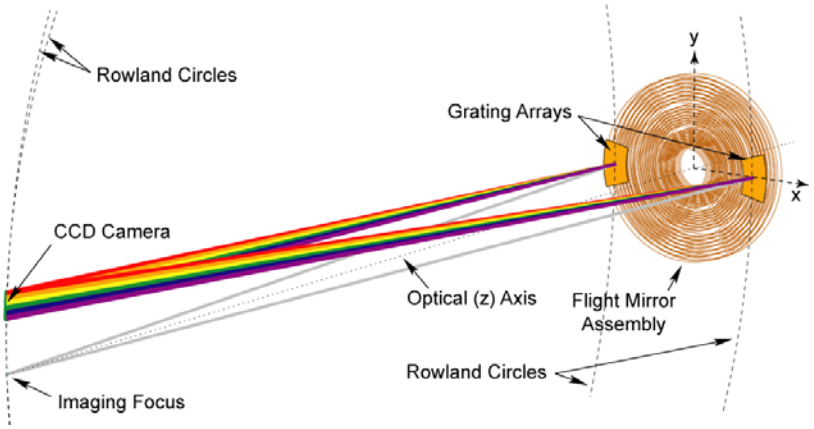

Figure 18: Geometry of the CAT grating dispersion

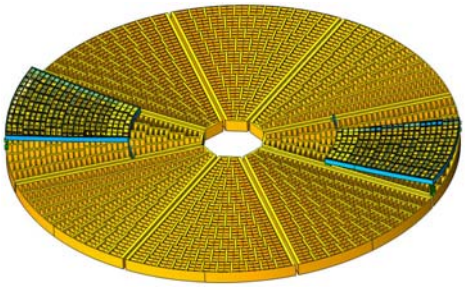

Figure 19: Configuration of the CAT gratings behind the silicon pore optics. Each of the grating assemblies cover 30° azimuth angle on the mirror.

The camera consists of a linear array of 32 CCDs (totaling a 25×780mm^2 detection area) and its housing (Camera Assembly), detector electronics and power supply (Detector Electronics Assembly - DEA), and the Digital Processing Assembly (DPA), containing the digital processor, all of which are mounted on the MIP.

Off-Plane Grating (OP-XGS)

The OP-XGS consists of an array of reflection gratings in the off-plane mount that diffracts light onto an array of dedicated CCDs [11]. Light intersects the surface of the grating at grazing incidence, 2.7°, and nearly parallel to the groove direction. This maximizes the illumination efficiency on the gratings. Furthermore, the groove profile can be blazed to preferentially diffract light to only one side of zero order thus increasing the efficiency further, see Figure 21. The blaze angle is chosen to maximize efficiency around 35 Å in first order (1 keV efficiency peaks in 3rd order) and is set to 12°. The off-plane geometry leads to diffraction along an arc at the focal plane. An advantage of this concept is the possibility to image the 0th order directly in the instrument, which eases the wavelength calibration.

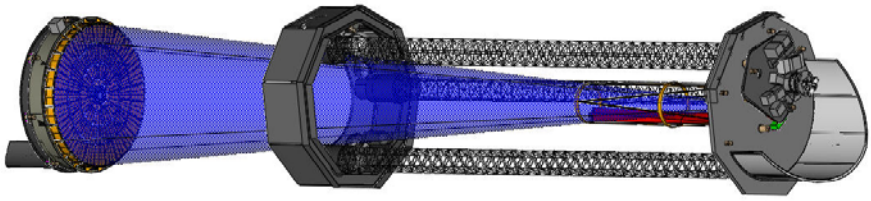

Figure 20: OP-XGS configuration on the spacecraft. The grating assembly is mounted on a tower fixed to the FIP. The drawing reflects the NASA design of the IXO spacecraft but the concept applies equally to the ESA design.

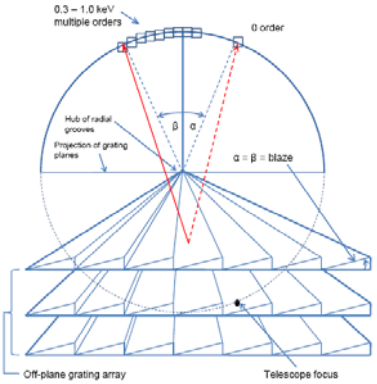

Figure 21: Geometry of the Off-plane grating dispersion.

A detailed trade-off study was performed to determine the optimal position of the gratings. The current design places them on a ~5 m tower fixed on the FIP, see Figure 20. Although this makes the accommodation more complex at the FIP level, the gratings would not require to be integrated with the mirror petals. The tower used for the gratings can also be used to accommodate the X-ray baffle and particle diverters needed for the on-axis instruments. The camera and its associated electronics are integrated into a single box and mounted on the FIP.

3.6 High-Time-Resolution Spectrometer (HTRS)

The HTRS will provide the International X-ray Observatory (IXO) with the capability of observing bright galactic X-ray sources (e.g. X-ray binaries, magnetars) [12]. Those sources can generate up to a million counts per seconds, equivalent to about 5 times the intensity of the Crab. The HTRS will further provide better than 200 eV spectral resolution at 6 keV, together with microsecond time resolution, for photons of energy between 0.3 and 10 keV. The HTRS is based on an array of 31 Silicon Drift Diodes (SDD) (Figure 22), placed out of focus, in a way that the focal beam is distributed over the whole array. SDDs rely on a depleted volume of silicon in which an arrangement of increasingly negatively biased rings drive the electrons generated by the impact of ionizing radiation towards a small readout anode located on the backside and in the centre of the device. The high charge carrier drift velocity and low capacitance of the readout node makes these detectors ideal to handle very high count rates simultaneously with good energy resolution.

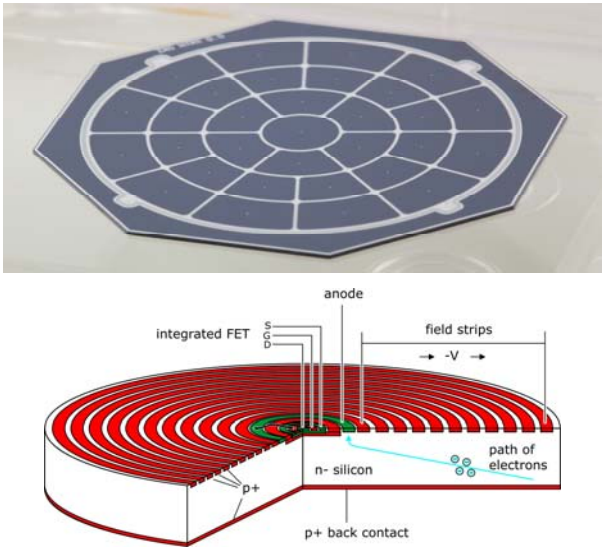

Figure 22: Detector prototype and pixel schematic

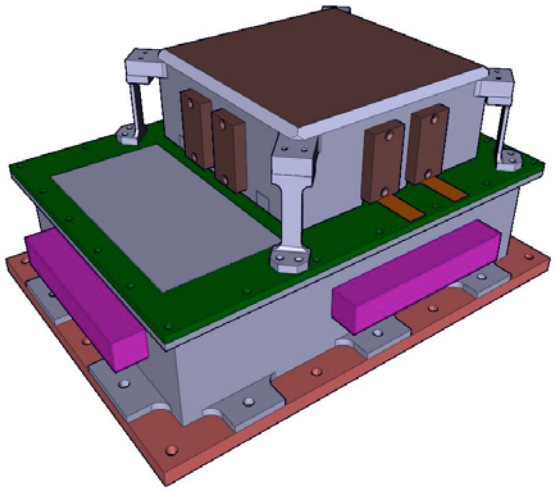

Figure 23: Detector assembly with front-end electronics

The detector is integrated together with the filter wheel and the front-end electronics into the focal plane assembly, Figure 23. An additional electronics unit is responsible for the configuration of the SDD array, the data acquisition, compression, storage, power conversion and interfaces with the spacecraft.

3.7 X-ray Polarimeter (XPOL)

XPOL is to provide, in the energy range 2 – 10keV, polarization measurements simultaneously with angular measurement (5 arcsec), spectral measurements (E/ΔE of ~5 @6 keV) and timing at a few μs level. XPOL is based on a Gas Pixel Detector (using Dimethyl-Ether), a counter with proportional multiplication and finely subdivided anode structure that is able to recognize tracks and hence to derive the ejection direction of the primary photoelectron, see Figure 24. The track analysis also provides the impact point with a precision of ~150 μm FWHM, largely oversampling the mirror PSF. The read-out chip is integrated in the gas cell and has 105600 anodes or pixels on a 50 μm pitch. The field of view is 2.6'×2.6'.

In addition to the focal plane assembly consisting of the detector, proximity electronics, filter wheel and polarized calibration source (Figure 25), the instrument includes two electronics units. The Back End Electronics (BEE) will manage the detector ASIC, supply the high voltages, implement a spectroscopy electronic chain for the GEM analog output, digitize the signals and perform some basic event processing (pedestal calculation, suppression of not-fired pixels). The Control Electronics (CE) is a data processing box which also controls the whole instrument.

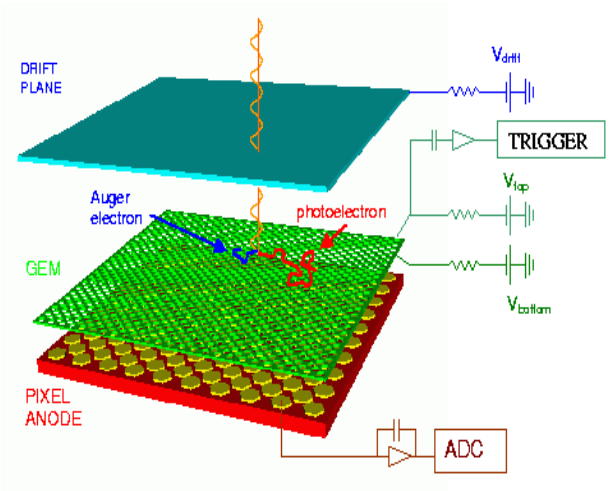

Figure 24: Gas cell principle of operation.

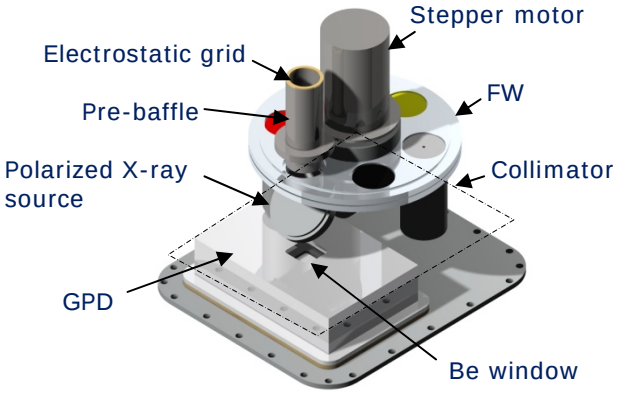

Figure 25: Gas Pixel Detector with filterwheel

4. RESOURCE REQUIREMENTS

A summary of the instruments' key characteristics is provided together with their resource requirements in Table 2.

Table 2: Summary of IXO instruments (mass and power including design maturity margins).

Instrument Characteristic	WFI&HXI Combined		XMS	HTRS	XPOL	XGS[1]
	WFI	HXI				
Detector type	Si APS (DEPFET)	CdTe + Si strip detectors	Micro-calor. (TES)	Silicon Drift Diodes	Gas Pixel Detector	CCD
Mass (kg)	101	28 129	392[2]	30	15	122
Peak Power (W)	283	56 339	1017[3]	145	55	137
Detector T_{ops}	210 K	233 K	50 mK	233 K	283 K	183K
Cooling	Radiator	Radiator	Closed cycle, ADR	Radiator	Peltier	Radiator
Detector Size (mm)	102.4 × 102.4	50 × 50	31.2 × 31.2	24 (circular)	15 × 15	786 × 24
Energy Range (keV)	0.1 – 15	10 – 40	0.3 – 12	0.3 – 15	2 – 10	0.3-1
Energy resolution (FWHM)	50 eV @ 282 eV 125 eV @ 6 keV	1 keV @ 40 keV	2.5 eV @ <6 keV	200 eV @ 6 keV	1200 eV @ 6 keV	E/ΔE > 3000
Pixel size (μm)	100	250	300 (& 600)[4]	3400	50	24
Pixels in one dimension	1024	192 strips	40 (+ 32)[4]	7	300	32768
Field of View (arcmin square)	17.6 × 17.6	8 × 8	2 × 2 (& 5.4 × 5.4)[4]	N/A	2.6 × 2.6	N/A
Typ/max data rate (kbps)	45/450	11/256	64/840	840/840	840/840	128/128 (1280)[5]

[1] Assuming the CAT grating option design for the Silicon Pore Optics Mirror
[2] Total of 113 kg for XMS instrument and 279 kg for the cryostat + cryo-cooler chain (ESA CDF baseline cooler)
[3] Total of 520 W for XMS instrument and 497 W for the cryo-cooler chain (ESA CDF baseline cooler)
[4] For inner and outer array respectively
[5] Peak rate for < 6 hr/month

ACKNOWLEDGEMENTS

The authors wish to acknowledge the work done by the various instrument consortia lead by MIT for CAT-XGS, Open University UK for OP-XGS, SRON Netherlands for XMS, CEA France for MIS-XMS, MPI Germany for WFI, ISAS/JAXA for HXI, CESR France for HTRS and INFN Italy for XPOL as well as EADS Astrium (study manager A. Russel), Thales Alenia Space (study manager Y. Roche) in the context of the parallel competitive industrial studies. The work performed at ESTEC by the CDF team proved very useful for the IXO assessment study. The support provided by the NASA and JAXA colleagues is also acknowledged together with the IXO Study Coordination Group, Instrument Working Group and Telescope Working Group.

REFERENCES

[1] Parmar A., Hasinger G. and Turner M., Proc 34th Cospar Assembly, p2368, (2004).
[2] Bookbinder J. et al, Proc. of SPIE 7011, (2008).
[3] Bignami G. et al, Cosmic Vision, ESA BR-247, (2005).
[4] Reference material available at http://ixo.gsfc.nasa.gov/resources/0209_Decadal_WhitePapers.html
[5] Instruments reference design document is available at the following link: http://sci.esa.int/sciencee/www/object/index.cfm?fobjectid=44697#
[6] Rando N., Martin D., Verhoeve P., et al., "ESA assessment study activities on the international X-ray observatory", SPIE, these proceedings (2010).
[7] Strüder L.W., "A wide dield imager for IXO: status and future activities", SPIE, these proceedings (2010).
[8] Nakazawa K., Takahashi T., Limousin O., et al., "The hard x-ray imager onboard IXO", SPIE, these proceedings (2010).
[9] Den Herder J.-W. A., Kelley R.L., Mitsuda K., et al., "The x-ray microcalorimeter spectrometer onboard of IXO", SPIE, these proceedings (2010).
[10] Heilmann R.K., Ahn M., Bautz M.W., et al., "Critical-angle transmission grating spectrometer for high-resolution soft x-ray spectroscopy on the International X-ray Observatory", SPIE, these proceedings (2010).
[11] McEntaffer R.L., Schultz T., Cash W.C., et al., "Developments of the off-plane x-ray grating spectrometer for the international X-ray Observatory", SPIE, these proceedings (2010).
[12] Barret D., Ravera L., Amoros C., et al., "The high time-resolution spectrometer of the International X-ray Observatory", SPIE, these proceedings (2010).